ARTICLE

Supplementary Information for

Quantifying chiral handedness of core-shell inorganic nanotubes via electron microscopy and diffraction

Kaiyuan Wang,[a] Beilynn Geiss,[b] Roy Geiss,[c] James R. Neilson,[a] Alla Zak,[d] Justin B. Sambur[a]

[a.] *Department of Chemistry, Colorado State University, 200 West Lake Street, Fort Collins, Colorado 80523-1872, United States.*
[b.] *Skidmore College, Saratoga Springs, New York 12866, United States.*
[c.] *Analytical Resources Core, Colorado State University, 200 West Lake Street, Fort Collins, Colorado 80523-1872, United States.*
[d.] *Faculty of Science, Holon Institute of Technology, Holon 5810201, Israel.*

*Corresponding Author:

E-mail: Justin.Sambur@colostate.edu

TEM Image Analysis Procedure.

FFT to IFFT image analysis approach. Figure S1 and Figure S5 illustrate the image analysis approach and the caption describes each step in the approach. First, a local region of an NT image (Figure S1a) is selected and transformed to reciprocal space by FFT (Figure S1b). In the FFT, the WS_2 lattice fringes appear as lines aligned along a direction that is perpendicular to the fringes seen in the TEM image. Next, the user can define a region of interest in the FFT image using the mask function in the Digital Micrograph software to select the band of reciprocal space frequencies that lie along the WS_2-related direction in the FFT (white regions in Figure S1). The circled spots in Figure S1b simply mark the WS_2-related direction; they are not the complete set of WS_2 frequencies. The mask retains the whole directional frequency band, since only the orientation is required for visualization. Lastly, applying the IFFT to the masked FFT to reconstruct a real-space image in which the WS_2 lattice orientation is clearly enhanced (Figure S1d).

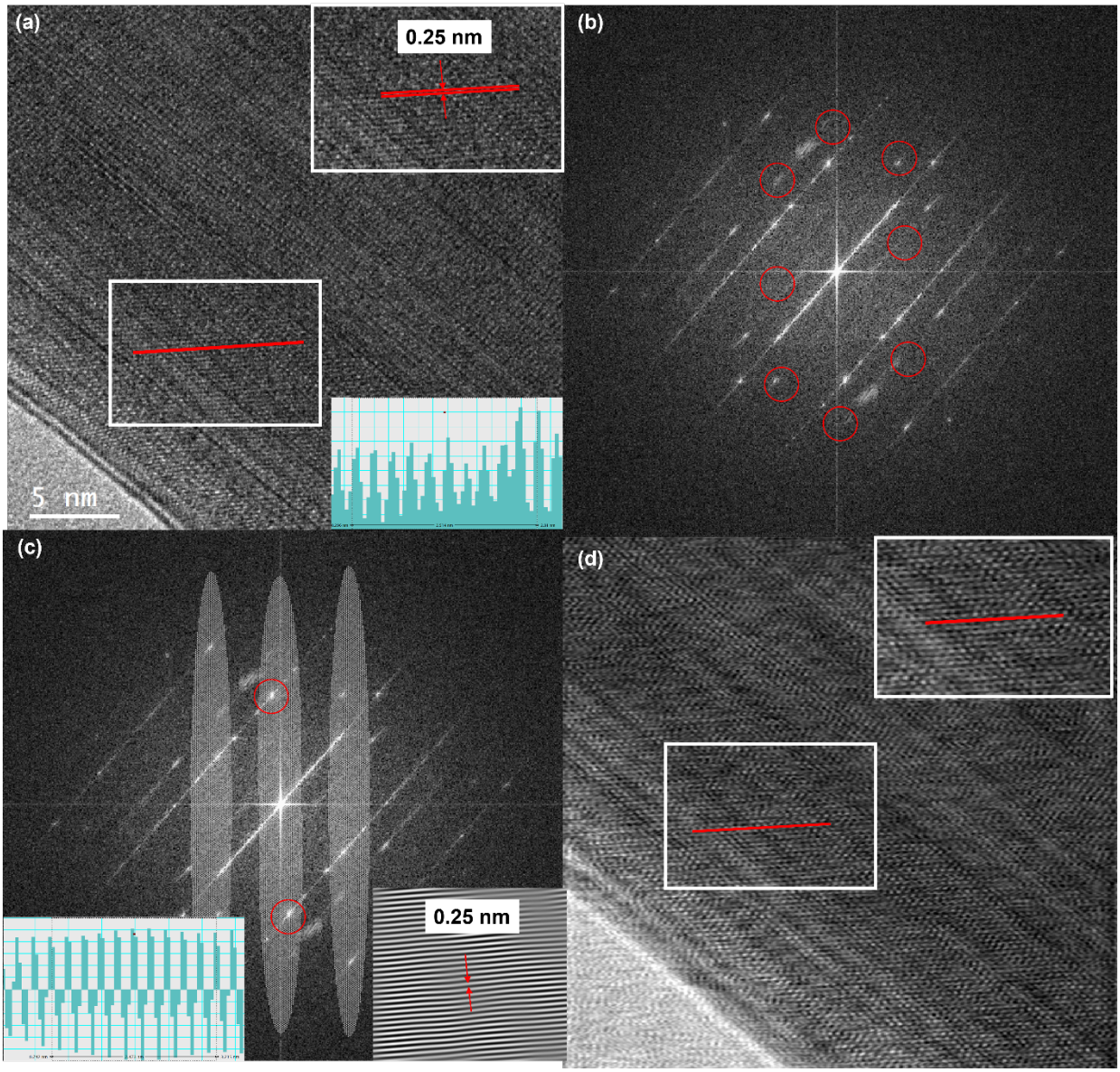

Figure S1. Identifying the WS_2 lattice fringes in TEM using Fast Fourier Transform (FFT) and Inverse Fast Fourier Transform (IFFT). **(a)** Selected area of the TEM image from Figure 5a in the main text. The inset shows a zoomed-in view of the WS_2 lattice (red line) indicated by the white box. The bottom right shows the line profile of the WS_2 lattice. **(b)** FFT image of panel (a), where the red circles indicate the WS_2-related FFT spots. **(c)** A user-defined region of interest (white regions), or mask, is placed on the FFT image perpendicular to the lattice fringes in real space. The bottom right is the IFFT image of the selected red circles in panel c, and the bottom left shows its line profile. A stripe-shaped mask was applied in the FFT to include both the WS_2 diffraction features and the elongated WO_x-related features. This approach allows the inverse FFT reconstruction to reflect the combined real-space periodicities of the WS_2 shell and WO_x core, consistent with the experimental TEM image. Filtering only the WS_2 spots would isolate the shell periodicity but would not reproduce the full core–shell structural contrast. **(d)** IFFT reconstructed image from the regions of interest in panel (c). The inset shows a zoomed-in view of the WS_2 lattice (red line) indicated by the white box.

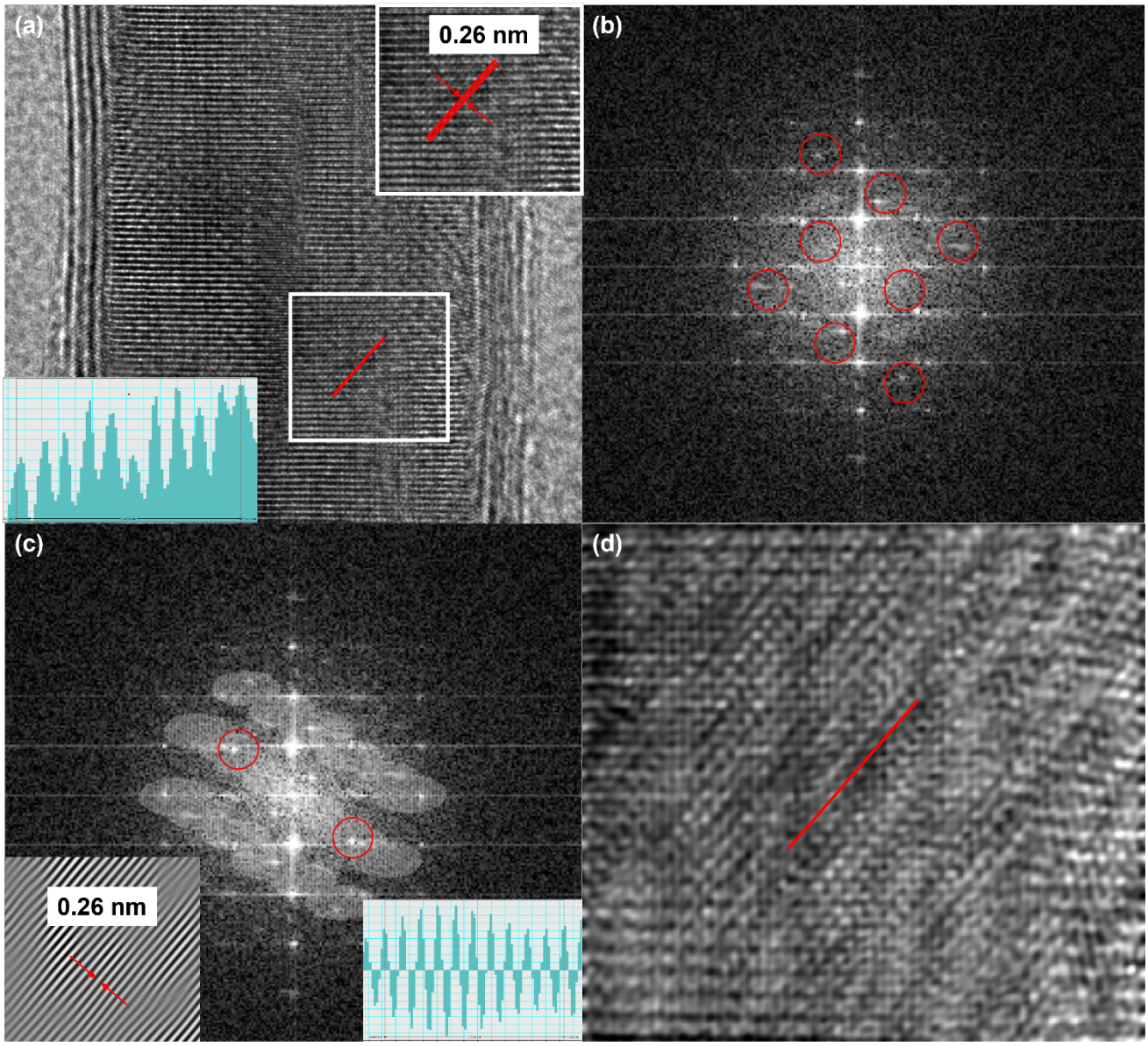

Figure S2. Identifying the WS_2 lattice in TEM using Fast Fourier Transform (FFT) and Inverse Fast Fourier Transform (IFFT). **(a)** Selected area of the TEM image from Figure 5b in the main text. The inset shows a zoomed-in view of the WS_2 lattice (red line) indicated by the white box. The bottom left shows the line profile of the WS_2 lattice. **(b)** The FFT image, where the red circles indicate the WS_2-related direction suggested in (a). **(c)** Mask and keep the area (white region) corresponding to the WS_2-related direction, which is perpendicular to the lattice fringes in real space. The bottom left is the IFFT image of the selected red circles in panel c, and the bottom right shows its line profile. **(d)** The IFFT reconstructed image shows the WS_2 lattice (red line).

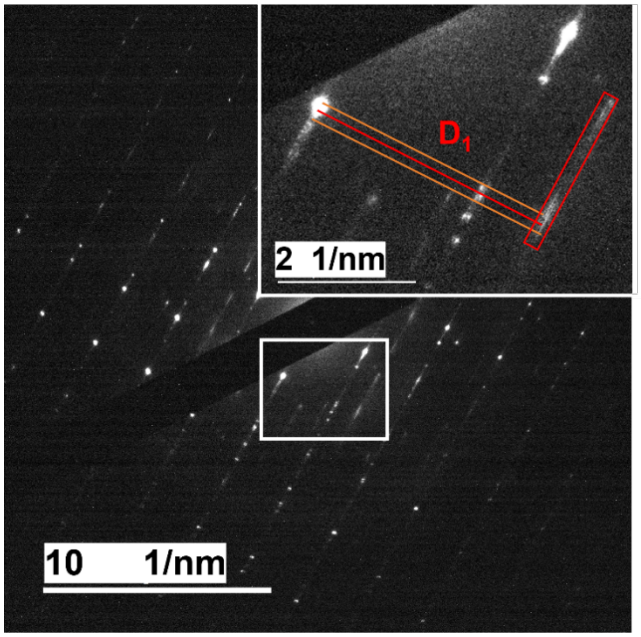

Figure S3. Measurement of the d-spacing in the SAED pattern. The d-spacing is defined as the distance between a diffraction line and the equatorial line. The inset shows a magnified view of the boxed region: orange lines mark the longest and shortest measured distances, and the red line indicates the averaged distance used in this work. The red box highlights the treatment of diffraction from multiple WS_2 shells as a single line.

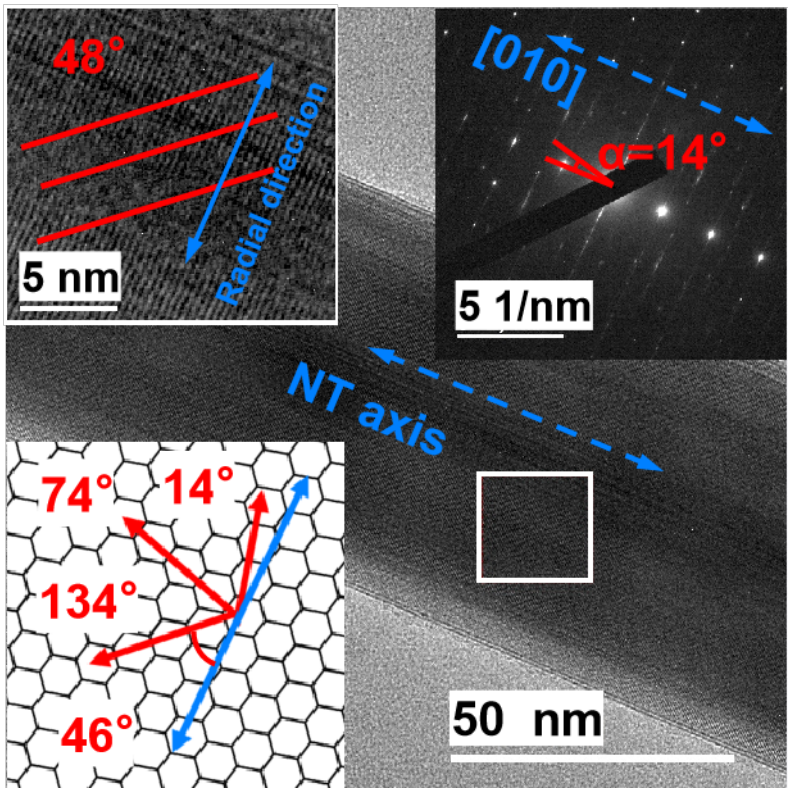

Figure S4. Another example of handedness identification. Insets (top-left) are a zoom-in view of the boxed TEM region, highlighting the 48° chiral angles (red) and (top-right) 14° chiral angles measured in its SAED pattern. The bottom left inset shows the reference frame that relates the TEM-derived angle in the lower right inset (48°) to the chiral angle measured via SAED.

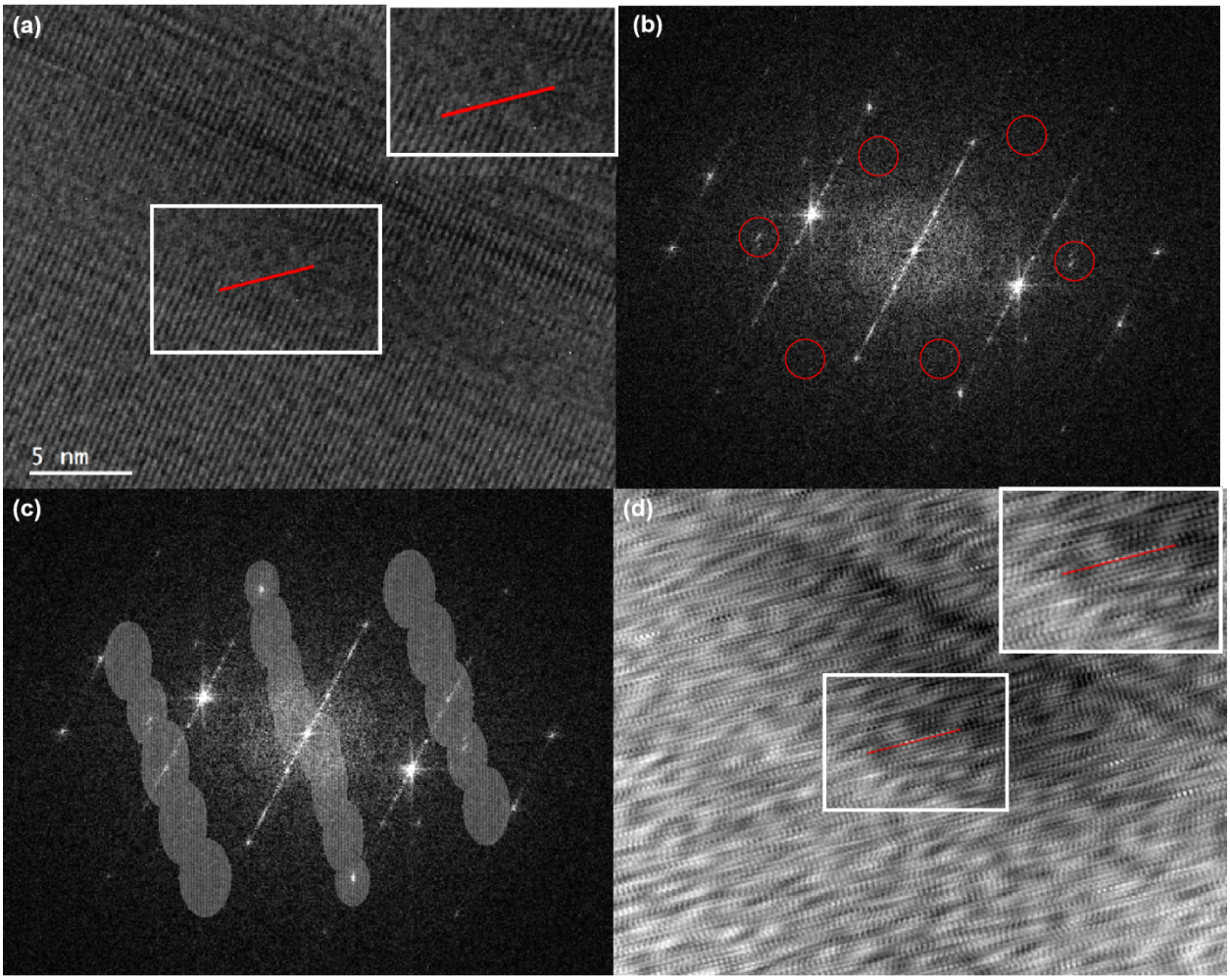

Figure S5. Identifying the WS_2 lattice in TEM using Fast Fourier Transform (FFT) and Inverse Fast Fourier Transform (IFFT). **(a)** Selected area of the TEM image from Figure S4. The inset shows a zoomed-in view of the WS_2 lattice (red line) indicated by the white box. **(b)** The FFT image, where the red circles indicate the WS_2-related direction suggested in (a). **(c)** Mask and keep the area (white region) corresponding to the WS_2-related direction, which is perpendicular to the lattice fringes in real space. **(d)** IFFT reconstructed image. The inset shows a zoomed-in view of the WS_2 lattice (red line) indicated by the white box.

Qualitative approach. Alternatively, lattice fringes may appear in TEM images as shown in Figure 3. Three main steps were used to qualitatively identify WS_2 lattice fringes in TEM images. First, we obtained TEM images and SAED patterns of a single NT. The SAED reflections exhibit slight elongation/broadening, which is commonly observed in nanotube diffraction due to curvature-induced orientation spread within the selected-area aperture. The chiral angle can be derived from the SAED pattern by measuring the D-spacings. The midpoint of the diffraction line should be taken as the endpoint (Figure S3) to generate an average value of all possible layers within a multiwalled NT. Two D-spacings (D_1 and D_2, or D_1 and D_3, or D_2 and D_3) are sufficient for calculating the chiral angle, and the relevant equations are provided in the main text.

Second, we identify the WS_2 lattice line in the TEM image that corresponds to the chiral angle measured from the SAED pattern. In some cases, this WS_2 line can be directly observed without a moiré pattern, while in other cases, the moiré pattern is observed (Figure S5). In such cases, the moiré pattern can serve as a guide: the WS_2 lattice lines run in the opposite direction to the moiré pattern. Consistency between the SAED-derived angle and the TEM image further verifies whether the observed lines correspond to the WS_2 lattice or to the moiré pattern, as shown in the reference frames in main text figures. Practical adjustments such as zooming in or out and slowly moving the figure can help to distinguish between the two.

Third, we determine the handedness based on the angle measured in the TEM image. If the angle is between 0° and 30°, the handedness follows the oriented direction of the lattice lines. For instance, a 15° left orientation indicates a left-handed NT. If the angle is between 30° and 60°, the handedness is opposite to the orientation direction (Figure 6). For example, a 45° left orientation indicates a right-handed NT.

An optional fourth step is to perform a simulation to further validate the assignment. Using the structure and parameters measured in TEM images, one can simulate the moiré pattern by overlapping the strip-like tungsten oxide and the hexagonal WS_2 lattice (Figure 6). This simulated pattern can then be directly compared with the experimental TEM images to check consistency.

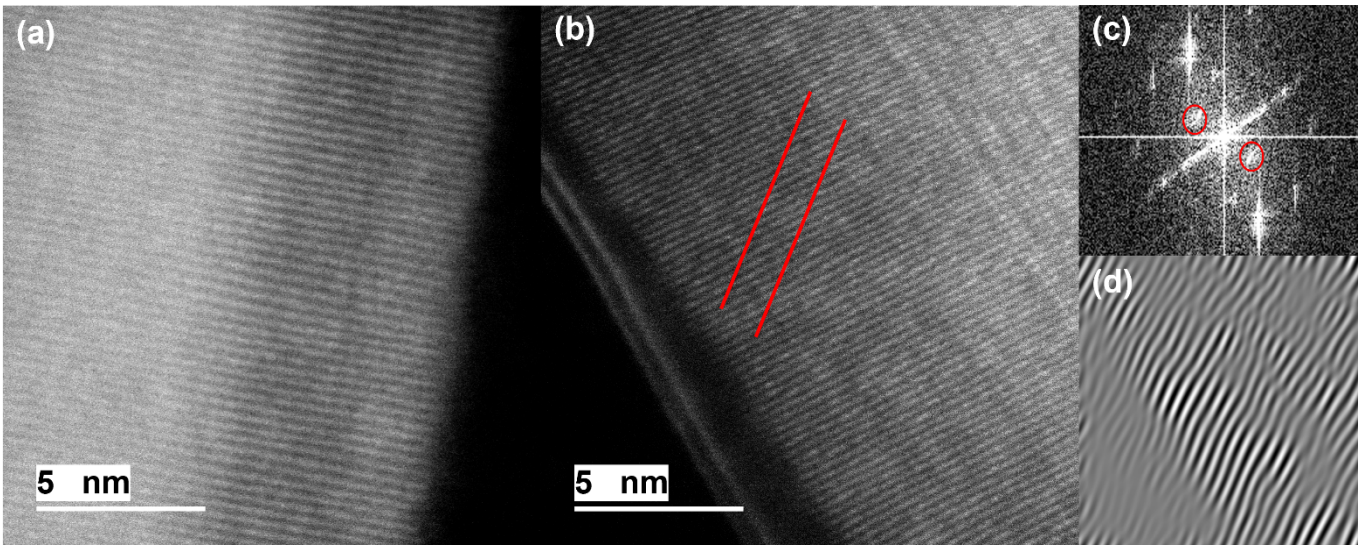

Figure S6. High-angle annular dark-field scanning transmission electron microscopy image of **(a)** a tungsten oxide rod without WS_2 layers, and **(b)** a multi-wall WS_2 NT with tungsten oxide core. The moiré patterns are indicated by red lines. **(c)** FFT of the moiré-pattern region in panel (b); the red circles highlight the moiré-related features. **(d)** Inverse FFT (IFFT) reconstruction using the circled features in panel (c).

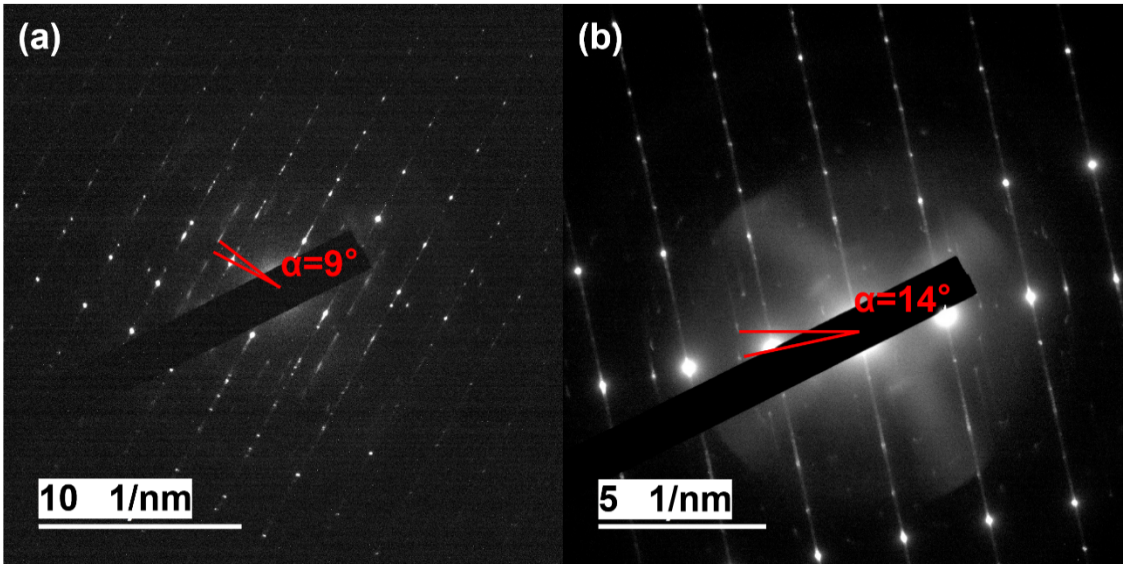

Figure S7. Chiral angles measured from the SAED patterns of **(a)** the WS_2 NT shown in Figure 6a and **(b)** the NT shown in Figure 6b. The number of diffraction lines corresponds to the number of WS_2 shells, with each shell contributing a slightly different chiral angle (typically differing by a few degrees). In this work, such minor inter-shell angular variations are neglected. Instead, the diffraction pattern is treated as a single effective line, and the average chiral angle is determined by measuring the distance between the equatorial line and the midpoint of the diffraction line.

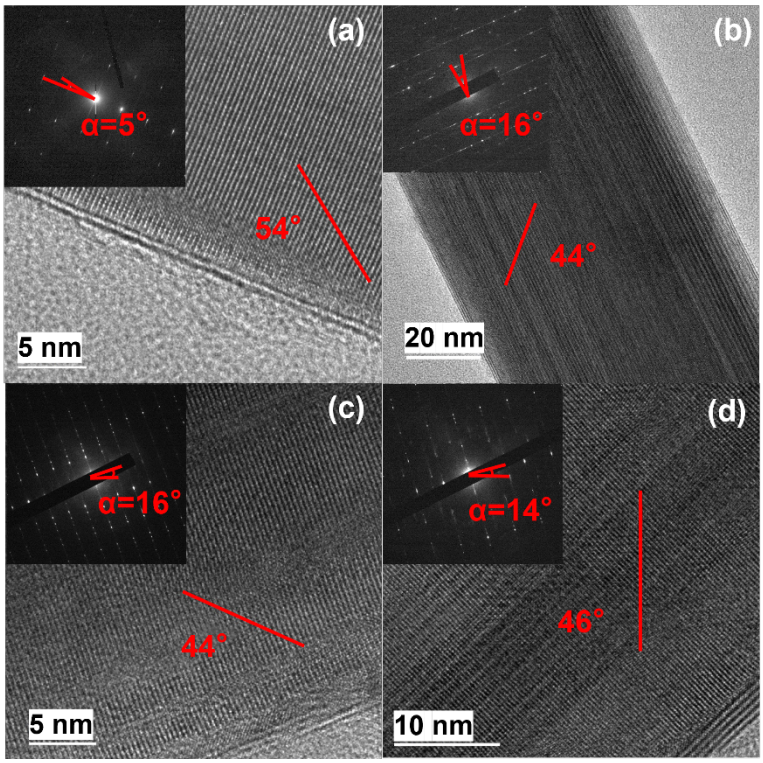

Figure S8. Four examples of handedness identification showing **(a)** left-handed with 5° chiral angles; **(b)** left-handed with 16° chiral angles; **(c)** left-handed with 16° chiral angles; **(d)** right-handed with 14° chiral angle.

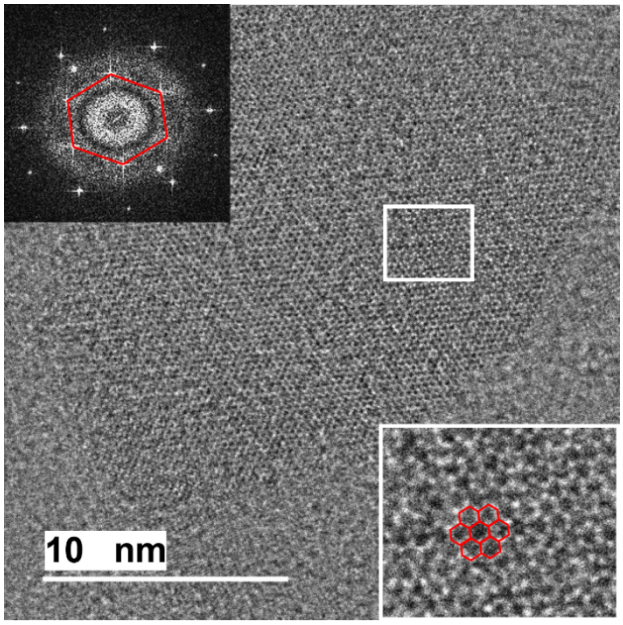

Figure S9. TEM image of a peeled-off WS_2 layer viewed along the [001] zone axis. Insets: (bottom right) a magnified view of the boxed region; (top left) the Fast Fourier Transform (FFT) calculated from a larger region of the same layer. The red marks highlight the hexagonal lattice.